Investigation of band inversion in (Pb,Sn)Te alloys using *ab initio* calculations

Xing Gao and Murray S. Daw
Department of Physics & Astronomy, Clemson University, Clemson, South Carolina 29634, USA
(Received 10 July 2007; published 17 January 2008)

The electronic structure of the (Pb,Sn)Te alloy displays the so-called "band inversion" between its two end members, PbTe and SnTe. Although the electronic structures of these two end members have been extensively studied by first-principles calculations, there have been no reports of first-principles calculations of the evolution of the band gap with composition. We have studied systematically the band structure using first-principles calculations within the generalized gradient approximation and have investigated the effects of compositional disorder. By taking into account local disorder, we show that the calculated dependence of band gap on composition is in good agreement with experimental results.

DOI: 10.1103/PhysRevB.77.033103 PACS number(s): 71.23.−k, 71.20.Nr

The rocksalt-structure IV-VI semiconductor compounds—such as PbTe, PbSe, PbS, and SnTe—have small band gaps, high dielectric constants, and a variety of very unusual thermodynamic, vibrational, electronic, and infrared properties.[1] These narrow band-gap semiconductors have been of great interest for the last 4 decades for their fundamental physics and their application in infrared devices and thermoelectric materials. In fact, PbTe was one of the first materials studied by Ioffe and his colleagues in the middle of the past century when there was a revival of interest in thermoelectricity.[2]

These rocksalt-structure semiconductors show a series of electronic anomalies relative to the usual II-VI semiconductors. For example, the direct band gap occurs at the L point in the Brillouin zone, while the direct gap in II-VI semiconductors occurs at the Γ point. Also, the order of the band gap $E_g(\mathrm{PbS}) > E_g(\mathrm{PbTe}) > E_g(\mathrm{PbSe})$ and the order of the valance band maximum (VBM) energies $\mathrm{E_{VBM}(PbS)} > \mathrm{E_{VBM}(PbSe)} > \mathrm{E_{VBM}(PbTe)}$ are anomalous compared to that of II-VI semiconductors, which show the opposite trend. Furthermore, the band-gap pressure coefficient of Pb chalcogenides is negative, again in contrast to II-VI materials.

Among these compounds, $\mathrm{Pb_{1-x}Sn_xTe}$ displays what has been called "band inversion," that is, the band gap of SnTe is "inverted" relative to PbTe. In the former, the gap occurs between a valence band maximum with $\mathrm{L_6^-}$ symmetry and the conduction band minimum with $\mathrm{L_6^+}$ symmetry, while in the latter it is the opposite. This phenomenon was elucidated by Dimmock, Melngailis, and Strauss[3] in 1966, who pointed out that a level-crossing phenomenon occurs with increasing x. According to Dimmock *et al.*, with increasing Sn composition the energy gap initially decreases as the $\mathrm{L_6^+}$ and $\mathrm{L_6^-}$ states approach each other, goes to zero at some intermediate composition where the two states become degenerate, and then increases, with the $\mathrm{L_6^+}$ state now forming the conduction band edge and the $\mathrm{L_6^-}$ state forming the valence band edge. The change in E_g with alloying is ascribed to the difference between the relativistic effects associated with Pb and Sn. This "band inversion" model is consistent with the observed variation of E_g with x and the change in the sign of the temperature and pressure coefficients of E_g in going from PbTe to SnTe.

There have been numerous theoretical investigations on the electronic structures of these IV-VI compounds[4–17] and of defects in these systems.[18–20] Among those studies, Wei and Zunger[14] have carried out extensive electronic structure calculations for lead chalcogenides using the local density approximation as implemented by the linearized augmented plane wave method and have argued that the above anomalous electronic features can be attributed to the occurrence of the Pb s band below the top of the valence band, setting up coupling and level repulsion at the L point. Most recently, Ahmad *et al.*[19] have extensively studied the electronic structure of defects in PbTe. However, the only theoretical studies in the band-gap evolution in SnTe-PbTe solid solution systems are the empirical tight-binding studies by Lent *et al.* in 1986[12] and Lee and Dow in 1987.[13]

In this Brief Report, we will discuss the results of our attempts to further the understanding of the band-gap evolution in the (Pb,Sn)Te alloy using *ab initio* electronic structure calculations. We will demonstrate that local compositional disorder plays an important role in the band-gap formation in the intermediate compositions. We will show that short-range disorder breaks degeneracies near the band edge, giving rise to the observed trends in band gap.

We employed the all-electron full-potential linearized augmented plane wave (FLAPW) plus local orbital method[21] incorporated in WIEN2K.[22] The generalized gradient approximation (GGA)[23] for the exchange correlation potential was adopted in our present study. Scalar relativistic corrections were included and spin-orbit coupling was implemented using a second variational procedure.[24] Convergence of the self-consistent iterations was performed using 1000 k points inside the first Brillouin zone of special quasirandom structures (SQSs) to within 10^{-5} Ry. For all the current studies, calculations were performed using the fully optimized lattice constants and relaxed ionic sites. The structural optimizations were performed using the projector augmented wave (PAW) approach as implemented in the Vienna *ab initio* simulation package (VASP).[25]

The random $\mathrm{Pb_{1-x}Sn_xTe}$ alloys are described using the "special quasirandom structures" (SQSs).[26] In the SQSs, the alloy is modeled by occupying the cation sites in a supercell with Pb and Sn atoms so that the first few structural correlation functions are closely matched to the values in an infinite random alloy. We have generated various SQS-N structures (with $N=8$, 16 per unit cell for the cation Pb/Sn sublattice) at composition $x=0.125$, 0.25, 0.5, 0.75, and 0.875 using the

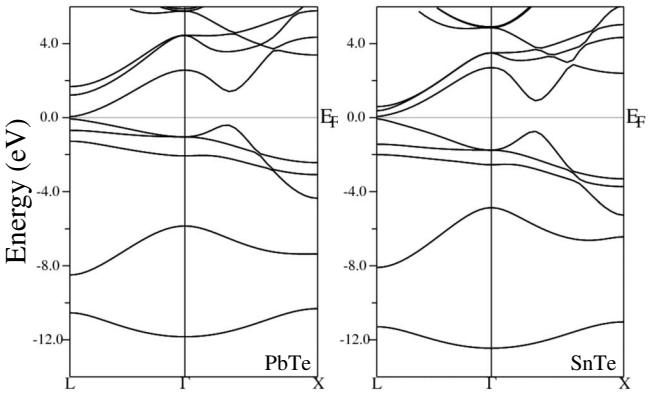

FIG. 1. Calculated relativistic band structures of pure PbTe and SnTe. The Fermi level is put in the center of the band gap. (For simplicity, the band structure for SnTe is displayed for the cubic phase. As noted in the text, the rhombohedral phase of SnTe is very slightly lower, and the rhombohedral distortion breaks the symmetry between the six L points, but only very slightly.)

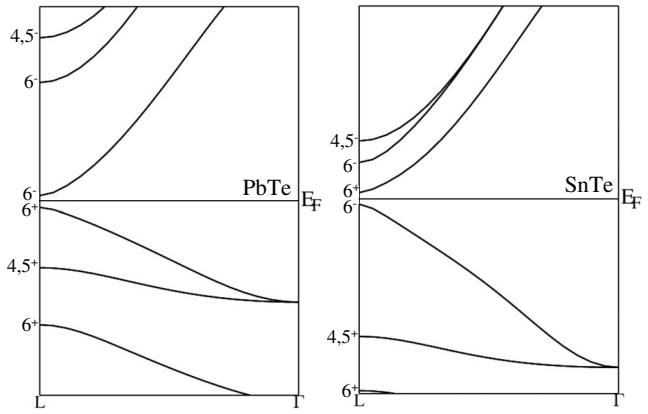

FIG. 2. Same as Fig. 1 but with expanded scale. Characters of the states at the L point are added.

gensqs code in the alloy-theoretic automated toolkit (ATAT).[27] For each composition x, our procedure can be described as follows: (1) Using *gensqs*, we exhaustively generate all structures based on the rocksalt lattice with $2N$ atoms per unit cell and given composition. (2) We then construct the pair correlation functions for each structure. (3) Finally, we search for the structure(s) that best match the pair correlation functions of random alloys, $(2x-1)^2$, up to sixth nearest neighbors. Then the selected SQSs were optimized with VASP.

We note experimental evidence that the Pb-rich alloys are cubic, while the alloys with more than 29% Sn content tend to a rhombohedral distortion.[28,29] Our calculations show that the rhombohedral phase of SnTe is indeed very slightly favored over the cubic phase—only by 0.4 meV *per SnTe pair*. In the cubic phase, the 6 L points are equivalent; the rhombohedral distortion breaks the degeneracy into sets of 4 and 2, and the band gap is reduced from 0.12 eV in the cubic structure to 0.09 eV in the rhombohedral structure. Overall, the energetics involved in rhombohedral distortion are so small, and the effect of the distortion on the bands is so weak, that it is not an important consideration in understanding the evolution of the band gap. Therefore in our following discussions we only focus on cubic and cubic-based structures. However, we note that our structures are *fully optimized* and structural distortions—including rhombohedral—in the alloys are permitted.

Before presenting the band-gap evolution in (Pb,Sn)Te as a function of alloy composition, we first briefly overview the basic physics of the band structures obtained from our current calculations, especially the band inversion between the two end members, PbTe and SnTe. For clarity of presentation, we have plotted the results using cubic SnTe; the slight rhombohedral distortion found in SnTe does not substantially alter the discussion. The calculated band dispersions along L-Γ-X and their characters at the L point are shown in Figs. 1 and 2, respectively. Our results are in good agreement with prior calculations.[8,14] Direct band gaps open at L in both systems. The band edges forming the gap have L_6^+ and L_6^- character in both compounds, but the order is "inverted" relative to each other. That is, the valence band maximum is L_6^+ in PbTe but L_6^- in SnTe (shown more clearly in Fig. 2). The L_6^+ state is mainly contributed by Pb/Sn s electrons plus Te p electrons, and the L_6^- state is mainly contributed by Pb/Sn p electrons plus Te s electrons. The calculated band gaps with GGA optimized lattice parameters are 0.12 eV for PbTe and 0.09 eV for rhombohedral SnTe (0.12 eV in its cubic case)—in reasonable agreement with the experimental results (0.18 eV for PbTe, 0.30 eV for SnTe at low temperature). It is noted here that the agreement for PbTe is better than that of SnTe. It is typical for LDA or GGA to underestimate band gaps; we find in the following calculations that the band gap is underestimated more on the Sn-rich side of SnTe-PbTe solid solutions.

We began by studying the band-gap evolution using *ordered* $Pb_{1-x}Sn_xTe$ structures, that is, Ca_7Ge type structure for $x=0.125$ and 0.875, $L1_2$ for $x=0.25$ and 0.75, and $L1_0$ for $x=0.50$. (Here, Ca_7Ge type structure, $L1_0$, and $L1_2$ are all referred to the Pb and Sn sublattice.) To understand more carefully what happens, we first consider the cases where there are no Sn substitutions in Ca_7Ge type structure, $L1_2$ and $L1_0$ PbTe. These structures are then simply the $2\times2\times2$ supercell of primitive PbTe, $1\times1\times1$ and $\frac{\sqrt{2}}{2}\times\frac{\sqrt{2}}{2}\times1$ conventional cells of rocksalt PbTe, respectively. Therefore, because of zone folding, the band gap of these structures should open at the Γ point of the Brillouin zone of the Ca_7Ge-type structure, at the R point $(\frac{1}{2},\frac{1}{2},\frac{1}{2})$ for the $L1_2$-type structure, and at the R point $(\frac{1}{2},0,\frac{1}{2})$ for the $L1_0$-type structure, respectively. The degeneracy at these ordered structures should be 16, 8, and 4, respectively. Incorporating Sn in these structures forming the *ordered* $Pb_{1-x}Sn_xTe$, we expect the band gap will open at the corresponding high symmetry points mentioned above if these ordered structures are semiconductors. The calculated band structures of these ordered structures are shown in Fig. 3. Clearly, at $x=0.25$ and 0.75 with $L1_2$ structures, and at $x=0.125$ and 0.875 with "Ca_7Ge-type structure," all systems are semimetals rather than semiconductors.

To illustrate why these ordered structures are not semiconducting, we show in Fig. 3 the characters of several

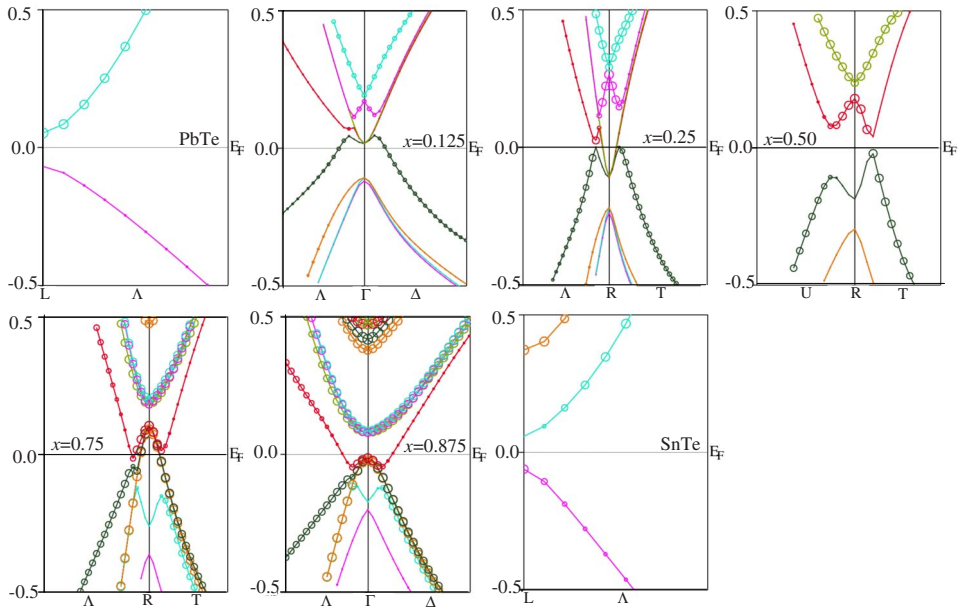

FIG. 3. (Color online) Calculated relativistic electronic structures of *ordered* (Pb,Sn)Te alloys (see text). Again, as in Fig. 2, band dispersions are shown on an expanded energy scale and also expanded in the wave vector for better clarity. The "fat" bands denote the contributions from Sn atoms (*s* and *p* orbitals) in ternary alloys. In the pure PbTe and SnTe systems, the "fat" bands denote contributions from Pb-*p* orbital and Sn-*p* orbital contributions, respectively. In all these figures, each single color represents one irreducible representation.

bands around the Fermi level using "fat" bands. Except the band inversion in the two end members, the Sn *s*- and *p*-like bands in these ordered structures are simply pushed upward above the Fermi level and the Pb *s*- and *p*-like bands are pushed downward below the Fermi level at the high symmetry points in all the ordered structures. Furthermore, some bands close to the Fermi level in Ca_7Ge-type structures and $L1_2$ structures are highly degenerate, resulting in the semimetal behavior in the band structures in these systems.

Having established that *ordered* Ca_7Ge-type structure and $L1_2$ and $L1_0$ structures do not represent the observed trends, we next hypothesize that the disorder expected in a solid solution will be important. The introduction of disorder *reduces* the symmetry of each structure, thereby breaking the degeneracy of the states near the Fermi level. In this way, disorder on the (Sn,Pb) sublattice creates band gaps in SnTe-PbTe solid solutions. It is noted that typically disorder introduces states in the gap, and that the present case is a counterexample. This is the central result of this work.

Here the SQS-8 structures are introduced to describe the disorder. The resultant band gaps are listed in Table I. We can see that compositional disorder does create the band gaps in these systems, and the trend of the band gap vs Sn composition compares well with both experimental results[3] and results obtained from model calculations for both cubic and rhombohedral phases with band structure parameters derived from the Shubnikov–de Haas study.[29] Careful study of the band characters of valence band maximum (VBM) and conduction band minimum (CBM) of these SQSs shows that the band inversion proceeds in the way as proposed by Dimmock *et al.* The resultant band characters are also listed in Table I. In Fig. 4 we compare our calculated band gap vs composition with the sketch of how this should happen from Dimmock *et al.* (Dimmock, Melngailis, and Strauss described the band inversion by using the unusual convention of a "negative band gap." Though the discussion of a "negative band gap" requires a little explanation, we have continued the practice because the trend of the band crossing is easy to display with this convention.) Our results are consistent with the hypothesis that local compositional disorder plays a role in the observed trends. Our estimated crossover is around $x=0.23$, at which the band gap is zero. This value is somewhat smaller than what Dimmock *et al.* proposed. It is also shown here that the band gap is underestimated more

TABLE I. The calculated band gaps and main contributions to the valence band maximum (VBM) and conduction band minimum (CBM) of SQS-8 structures.

	Main contribution		Band gaps (eV)	
Concentration *x*	VBM	CBM	Calculated	Expt./Interpolated
PbTe	Pb-*s* and Te-*p*	Pb-*p* and Te-*s*	0.12	0.18
0.125	(Pb,Sn)-*s* and Te-*p*	(Pb,Sn)-*p* and Te-*s*	0.06	0.12
0.25	(Pb,Sn)-*p* and Te-*s*	(Pb,Sn)-*s* and Te-*p*	0.013	0.05
0.50	(Pb,Sn)-*p* and Te-*s*	(Pb,Sn)-*s* and Te-*p*	0.022	0.08
0.75	(Pb,Sn)-*p* and Te-*s*	(Pb,Sn)-*s* and Te-*p*	0.11	0.20
0.875	(Pb,Sn)-*p* and Te-*s*	(Pb,Sn)-*s* and Te-*p*	0.10	0.25
SnTe	Sn-*p* and Te-*s*	Sn-*s* and Te-*p*	0.12	0.30

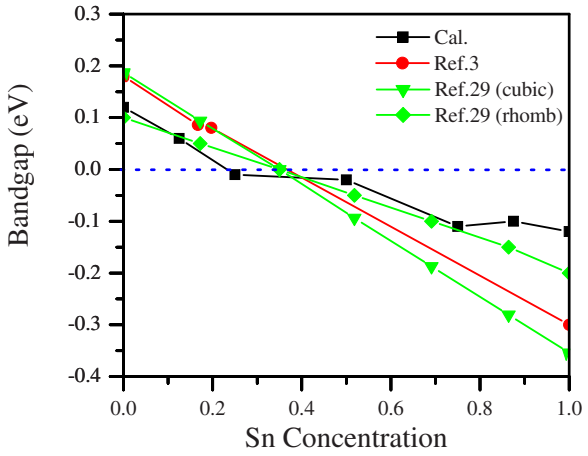

FIG. 4. (Color online) The calculated band gaps vs Sn concentration compared with an interpolation of the experimental results from Refs. 3 and 29. Following the convention set by other authors in prior publications, the crossing of levels which form the band edges is plotted in terms of a "band inversion," in which the band gap is depicted as going negative. The negative trend of the band gap with composition originates with the interchange of band edge symmetry. See Table I for greater detail.

on the Sn-rich side than that on the Pb-rich side.

It is noted that SQS-8 approximates only short-range disorder, but because the cell is periodic there is, in fact, a long-range order. By using a larger cell (going to SQS-16) we can increase the range of the short-range disorder. In Fig. 5, we compare the density of states of $Pb_{0.75}Sn_{0.25}Te$ with SQS-8 and SQS-16 structures. We can see that further increase in the range of the local disorder does not substantially change the electronic structure. This indicates that long-range interactions do not play a significant role in determining the band gap, which is consistent with the underlying assumption of the SQS approach.

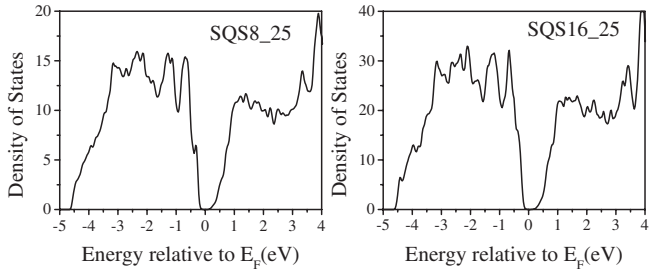

FIG. 5. The total density of states (DOS) per unit cell for SQS-8 and SQS-16 at Sn concentration of 0.25, demonstrating that the DOS is not significantly changed by going to a larger SQS cell.

In conclusion, the band-gap evolution in (Pb,Sn)Te through the range of composition was studied by first-principles GGA calculation, using SQS. It is shown that the local disorder plays an important role in the band-gap formation in the intermediate composition. Introducing short-range disorder into this system breaks the degeneracies near the band edge and produces a semiconducting behavior, which is in agreement with the experimental results. The calculated band gaps and the trend vs composition are in reasonable agreement with experimental results. The estimated crossover concentration is also in reasonable agreement with experimental results.

This work was supported by the Department of Energy under Grant No. DE-FG02-04ER-46139.

[1] G. Nimtz and B. Schlicht, *Narrow Gap Semiconductors*, edited by G. Hohler, Springer Tracts in Modern Physics Vol. 98 (Springer-Verlag, Berlin, 1983), p. 1.
[2] A. F. Ioffe, *Semiconductor Thermoelements and Thermoelectric Cooling* (Infosearch, London, 1957).
[3] J. O. Dimmock *et al.*, Phys. Rev. Lett. **16**, 1193 (1966).
[4] J. B. Conkin *et al.*, Phys. Rev. **137**, A1282 (1965).
[5] P. J. Lin and L. Kleinmann, Phys. Rev. **142**, 478 (1966).
[6] S. Rabii, Phys. Rev. **167**, 801 (1968); **182**, 821 (1969).
[7] F. Herman *et al.*, J. Phys. Colloq. **29** (Suppl.), C4-62 (1968).
[8] Y. W. Tang and M. L. Cohen, Phys. Rev. **180**, 823 (1969); Phys. Rev. B **3**, 1254 (1971).
[9] D. D. Buss and N. J. Parade, Phys. Rev. B **1**, 2692 (1970).
[10] S. E. Kohn *et al.*, Phys. Rev. B **8**, 1477 (1973).
[11] G. Martinez *et al.*, Phys. Rev. B **11**, 651 (1975).
[12] C. S. Lent *et al.*, Superlattices Microstruct. **2**, 491 (1986).
[13] S. Lee and J. D. Dow, Phys. Rev. B **36**, 5968 (1987).
[14] S. H. Wei and A. Zunger, Phys. Rev. B **55**, 13605 (1997).
[15] A. Delin *et al.*, Int. J. Quantum Chem. **69**, 349 (1998).
[16] M. Lach-hab *et al.*, J. Phys. Chem. Solids **61**, 1639 (2000).
[17] E. A. Albanesi *et al.*, Phys. Rev. B **61**, 16589 (2000).
[18] S. D. Mahanti and D. Bilc, J. Phys.: Condens. Matter **16**, S5277 (2004).
[19] S. Ahmad *et al.*, Phys. Rev. B **74**, 155205 (2006), and references therein.
[20] S. Ahmad *et al.*, Phys. Rev. Lett. **96**, 056403 (2006).
[21] D. J. Singh, *Planewaves, Pseudopotentials and the LAPW Method* (Kluwer Academic, Boston, 1994).
[22] P. Blaha *et al.*, *WIEN2k, An Augmented Plane Wave + Local Orbitals Program for Calculating Crystal Properties*, edited by K. Schwarz (Technische Universitat Wien, Vienna, Austria, 2001).
[23] J. P. Perdew *et al.*, Phys. Rev. Lett. **77**, 3865 (1996).
[24] D. D. Koelling and B. Harmon, J. Phys. C **13**, 6147 (1980).
[25] G. Kresse and J. Hafner, Phys. Rev. B **47**, 558 (1993); **49**, 14251 (1994); G. Kresse and J. Furthmuller, *ibid.* **54**, 11169 (1996); Comput. Mater. Sci. **6**, 15 (1996).
[26] A. Zunger *et al.*, Phys. Rev. Lett. **65**, 353 (1990).
[27] A. van de Walle, M. Asta, and G. Ceder, CALPHAD: Comput. Coupling Phase Diagrams Thermochem. **26**, 539 (2003).
[28] M. Iizumi *et al.*, J. Phys. Soc. Jpn. **38**, 443 (1975); S. Sugai *et al.*, Solid State Commun. **24**, 407 (1977); A. D. C. Grassie *et al.*, J. Phys. C **12**, L925 (1979); T. Suski *et al.*, *Phonon and Electrical Resistivity Anomalies at the Displacive Phase Transition in* $Pb_{1-x}Sn_xTe$ *and* $Pb_{1-x}Ge_xTe$, edited by E. Gornik, H. Heinrich, and L. Palmetshofer, Lecture Notes in Physics Vol. 152 (Springer-Verlag, Berlin, 1982), p. 266.
[29] He Yusheng and A. D. C. Grassie, J. Phys. F: Met. Phys. **15**, 317 (1985); **15**, 337 (1985); **15**, 363 (1985).